Supporting Information

Facile Method for Preparation of Three-Dimensional CNT Sponge and Nanoscale Engineering Design for High Performance Fiber-Shaped Asymmetrical Supercapacitors

Yong Li,[a] Zhuo Kang,[a] Xiaoqin Yan,*[a] Shiyao Cao,[a] Minghua Li,[a] Yichong Liu,[a] Shuo Liu,[a] Yihui Sun,[a] Xin Zheng,[a] and Yue Zhang*[ab]

a. State Key Laboratory for Advanced Metals and Materials, School of Materials Science and Engineering, University of Science and Technology Beijing, Beijing 100083, People's Republic of China.

b. Beijing Municipal Key Laboratory of New Energy Materials and Technologies, University of Science and Technology Beijing, Beijing 100083, People's Republic of China.

E-mail: xqyan@mater.ustb.edu.cn (X. Yan), yuezhang@ustb.edu.cn (Y. Zhang).

1. Experimental Section

2. Supplementary Figures

Figure S1. SEM images of 3DCS/P materials fibers with different PANI deposition cycles. (a) 3DCS/P2; (b) 3DCS/P3; (c) 3DCS/P4; (d) 3DCS/P5.

Figure S2. The relationship of the mass of 3DCS/P electrodes and deposition cycles.

Figure S3. Figure S3. Electrical conductivity of the fibers. (a) Schematic illustration of electrical conductivity measurements using a two-probe method. (b) I-V curves, (c) the calculated electrical resistance and (d) room-temperature electrical conductivity of the pristine CNT fiber, 3DCS fiber, 3DCS/P2, 3DCS/P3, 3DCS/P4 and 3DCS/P5.

Figure S4. XPS analysis of 3DCS/P samples.

Figure S5. CV and GCD curves of 3DCS/P electrodes. (a, b) 3DCS/P2; (c, d) 3DCS/P4; (e, f) 3DCS/P5.

Figure S6. Equivalent circuit for a 3DCS/P electrodes system.

Figure S7. (a) Impedance plot for a common electrochemical system, regions of mass-transfer and kinetic control are found at low and high frequencies, respectively. (b) Three different situations for a specified electrochemical system.

Figure S8. (a) The CV curves of 3DCS/P//3DCS FASC device measured at different potential window at 20 mV s^{-1}. (b) Comparative GCD curves of FASC device at different potential window ranges.

Figure S9. (a) CV and (b) GCD curves for two FASCs connected in series and parallel.

Figure S10. Leakage current curves of the FASC device charged to floating potential of 1.4 V and kept for 1 h.

Figure S11. Specific capacitance based on the area and mass of the 3DCS/P3//3DCS FASC device versus current density.

Figure S12. Ragone plot of 3DCS/P3//3DCS FASC device: E_i and P_i based on the total mass of the two electrodes and compares performance with those for the other fiber-shaped SCs.

Figure S13. Photo of homemade integrated system for mechanical stability and electrochemical stability test.

3. Supplementary Tables

Table S1. Comparison of electrochemical performance for previous reported carbon/PANI composites.

Table S2. Comparison of the equivalent series resistance (ERS) for previous reported fiber-shaped supercapacitors.

Table S3. Electrochemical performances of recently reported fiber-shaped SCs.

1. Experimental Section

Fabrication of 3DCS: Carbon nanotube fibers were directly prepared through in situ shrinking a CNT film with water and the CNT film was synthesized by an improved CVD method as reported previously.[45,46] The pristine CNT fibers were cut into 3 cm and held at one end with copper foil. Electrochemical activation was used to oxidize pristine CNT fibers in 1 M H_2SO_4 aqueous solution to produce the desired 3DCS. The electrochemical process was carried out in a three-electrode system with a pristine CNT fiber as the working electrode, an Ag/AgCl electrode as the reference electrode and Pt as the counter electrode. The activating process was carried out with the CV method between 1 and 2 V, the scan rate was 50 mV/s. The whole process of electrochemical activation was carried out at room temperature for 15 minutes, and the obtained CNT hydrogel fiber was washed with deionized water several times and stored in a glass vial containing deionized water. In order to maintain the porous structure of the CNT hydrogel, we used a freeze dryer to evaporate the internal moisture to obtain 3DCS.

Fabrication of 3DCS/PANI: 3DCS/P nanocomposites were synthesized by in situ electro-polymerization. Aniline monomer (AN, 3.73 g) was added to 80 mL of 1 M H_2SO_4 aqueous solution and then magnetic stirred for 20 min to ensure complete dispersion. The *in situ* polymerization was carried out in a three-electrode system with an obtained 3DCS fiber as the working electrode, an Ag/AgCl saturated electrode as the reference electrode and Pt as the counter electrode. The *in situ* electro-polymerization of PANI around the individual CNTs via cyclic voltammetry with the voltage of -0.2 to 0.8 V at a scan rate of 100 mV s^{-1}. The whole process of *in situ* electro-polymerization was carried out at 50 °C with different CV cycles. The samples with 200, 300, 400 and 500 CV cycles are denoted as 3DCS/PANI2, 3DCS/PANI3, 3DCS/PANI4 and 3DCS/PANI5, respectively. After polymerization, the as prepared 3DCS/PANI fibers were washed with de-ionized water and then dried at 80 °C for over 1 h.

Assembly of The FASC: The flexible all-solid-state fiber-shaped supercapacitors were fabricated by intertwining the prepared 3DCS/P electrode and a 3DCS fiber electrode, which serve as positive and negative electrodes, respectively. Both the positive and negative electrodes were pre-coated with a H_2SO_4-PVA gel polyelectrolyte before they were intertwined together. The H_2SO_4-PVA gel electrolyte was simply made as follows: in a typical progress, 6 g H_2SO_4 was mixed with 60 mL deionized water and then 6 g PVA powder was added. The whole mixture was heated up steadily to ~90 °C under vigorous magnetic stirring until the solution became clear. The intertwined electrodes were packaged spontaneously after the H_2SO_4-PVA gel solidified, and the all-solid-state fiber-shaped SC was prepared.

Material Characterization: The microstructures of 3DCS and 3DCS/P samples were conducted with field-emission scanning electron microscopy (FESEM, FEI Quanta 3D). X-ray diffraction patterns were collected on a Smartlab diffractometer equipped with Cu Kα radiation (λ = 1.5406 Å). Surface elements of electrode materials were investigated by X-ray photoelectron spectroscopy (XPS, VG Scientific ESCA-Lab220i-XL), using 300 W Al Kα radiation as an exciting X-ray source. The base pressure was about 3×10^{-9} mbar. The binding energies were referenced to the C 1s line at 284.8 eV from adventitious carbon. The Raman spectra were recorded on a LabRam-1B Raman spectroscope with He-Ne laser excitation at 532 nm.

Electrochemical Measurements: All the electrochemical performances were measured on a CHI 660E electrochemical workstation at room temperature. A three electrode system was used to measure the electrochemical performance of the individual electrode in 1 M H_2SO_4 aqueous solution

with an Ag/AgCl as the reference electrode and Pt as the counter electrode, respectively. The electrochemical properties of FASCs were tested by a two electrode method. The EIS of the electrodes were tested in the frequency range from 100 kHz to 10 mHz at open circuit voltage by applying a 5 mV signal. The Nyquist plot of the FASC was performed in the open voltage circuit potential of 0.015 V and amplitude of 5 mV.

The length specific capacitance of a single electrode in the three electrode cell was calculated from the galvanostatic charge/discharge (GCD) curves by the following equation

$$C_l = (I\Delta t)/(l\Delta V) \tag{1}$$

Gravimetric specific capacitance of a single electrode in the three electrode cell was calculated from the GCD curves according to equation

$$C_m = (I\Delta t)/(m\Delta V) \tag{2}$$

where I is the discharge current density (A), l is the length of the electrode, ΔV is the potential window (V), Δt is the discharge time (s) and m is the mass of the single electrode.

The area specific capacitance of the whole FASC in two electrode system was obtained by the equation

$$C_S = (I\Delta t)/(S\Delta V) \tag{3}$$

The mass specific capacitance of the whole FASC in two electrode system was obtained by the equation

$$C_M = (I\Delta t)/(M\Delta V) \tag{4}$$

Where S ($S = 2\pi rL$, r represent the radius of the electrode) is the surface area of the electrode, M $(M = m_+ + m_-)$ is the total mass of the positive and negative electrodes. By the area specific capacitance or mass specific capacitance to calculate the corresponding area or mass energy density (Wh cm^{-2}, Wh Kg^{-1}) and power density (W cm^{-2}, W Kg^{-1}).

$$E_i = \left(C_i\Delta V^2\right)/(2 \times 3.6) \tag{5}$$

$$P_i = 3600E_i/\Delta t \tag{6}$$

2. Supplementary Figures

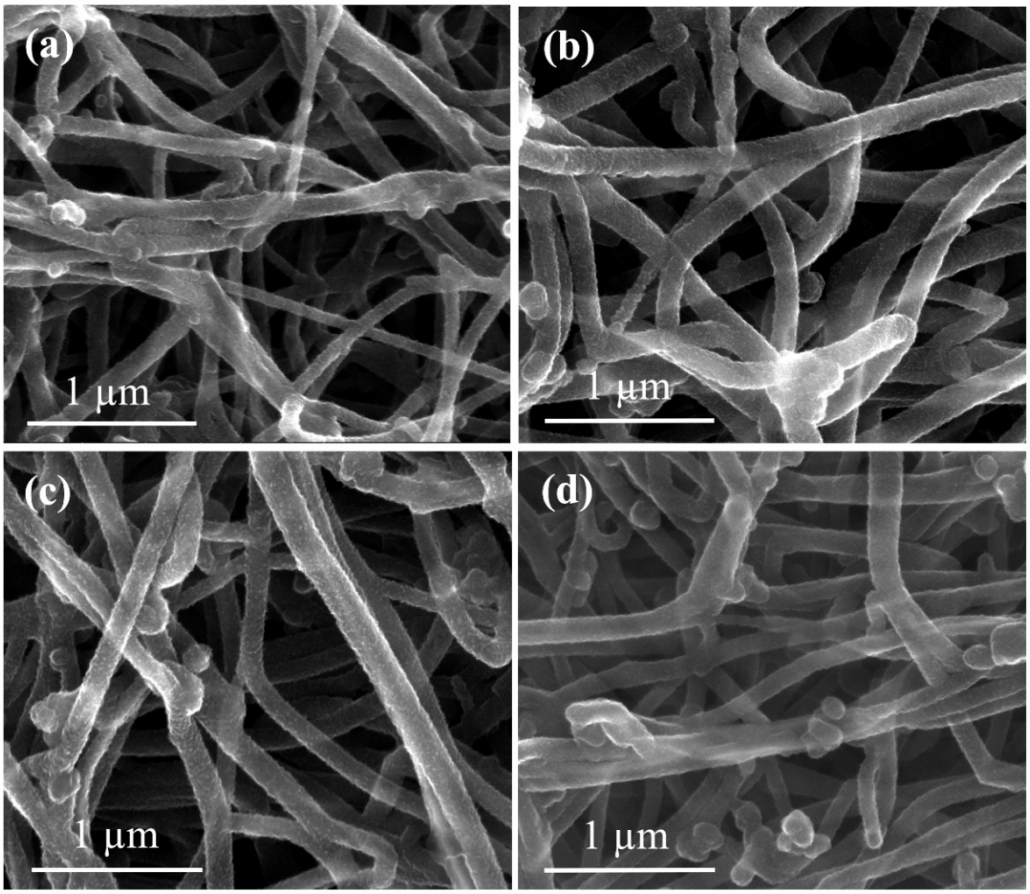

Figure S1. SEM images of 3DCS/P electrodes with different PANI deposition cycles. (a) 3DCS/P2, (b) 3DCS/P3, (c) 3DCS/P4, (d) 3DCS/P5.

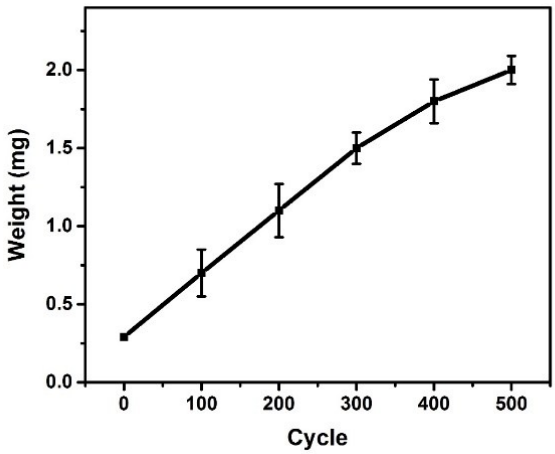

Figure S2. The relationship of the mass of 3DCS/P electrodes and deposition cycles.

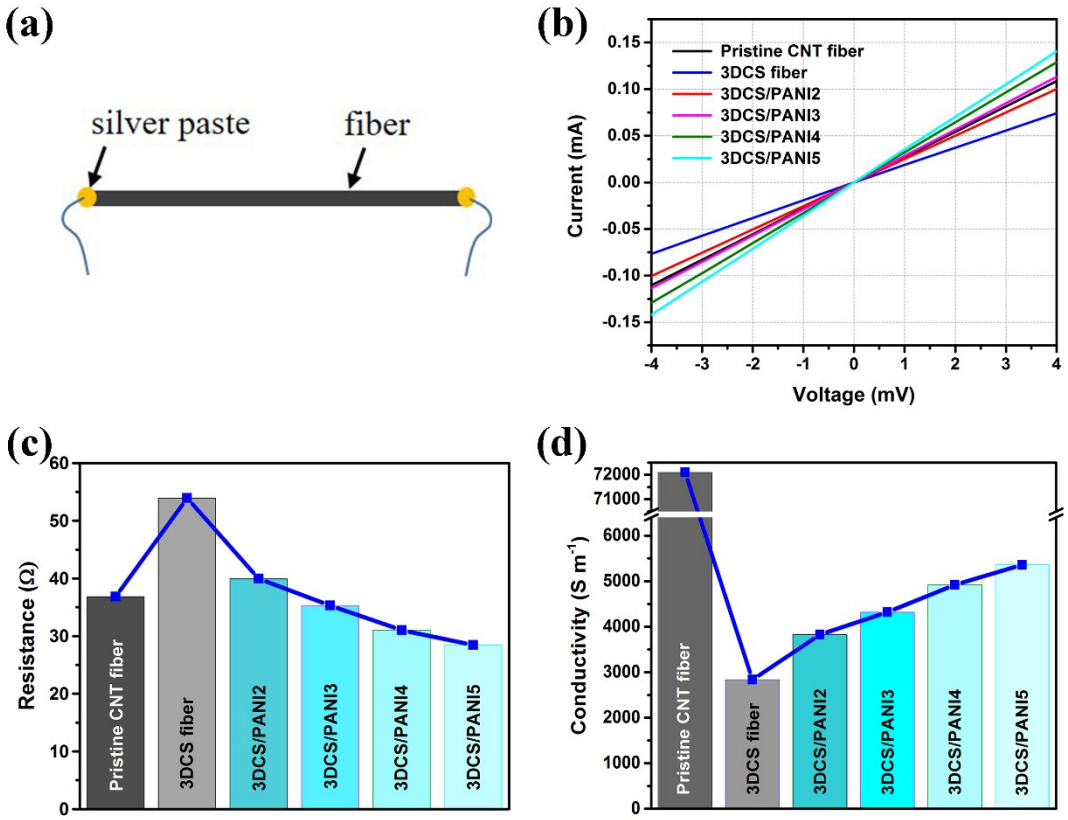

Figure S3. Electrical conductivity of the fibers. (a) Schematic illustration of electrical conductivity measurements using a two-probe method. (b) I-V curves, (c) the calculated electrical resistance and (d) room-temperature electrical conductivity of the pristine CNT fiber, 3DCS fiber, 3DCS/P2, 3DCS/P3, 3DCS/P4 and 3DCS/P5.

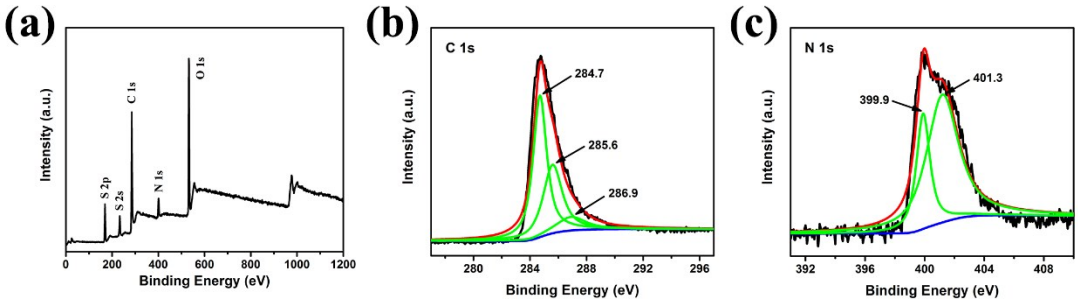

Figure S4. XPS analysis of 3DCS/P3 samples.

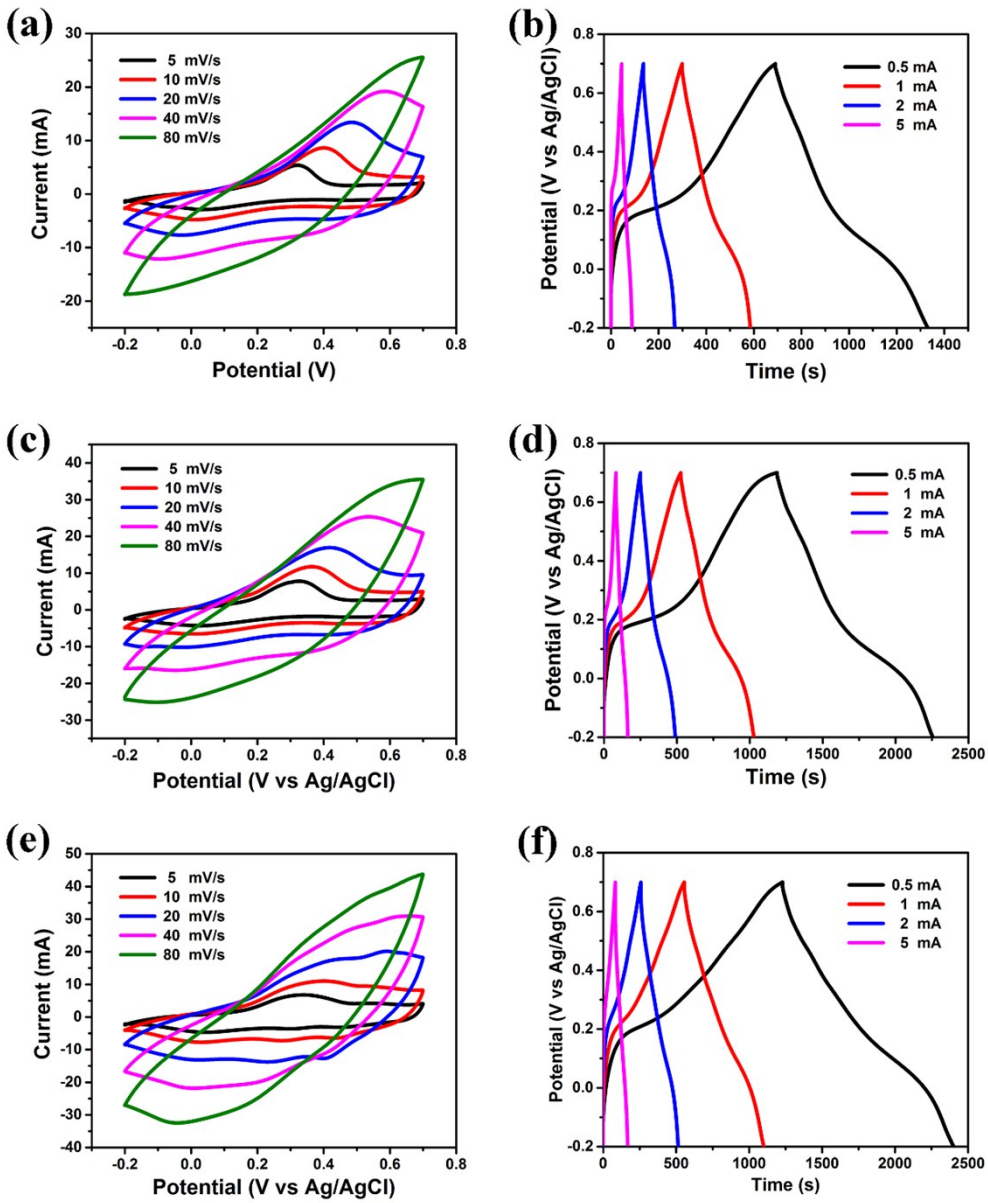

Figure S5. CV and GCD curves of 3DCS/P electrodes. (a, b) 3DCS/P2; (c, d) 3DCS/P4; (e, f) 3DCS/P5.

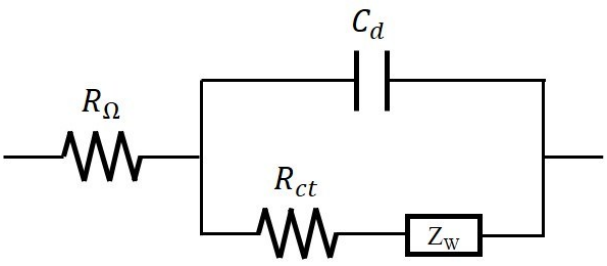

Figure S6. Equivalent circuit for a 3DCS/P electrodes system.

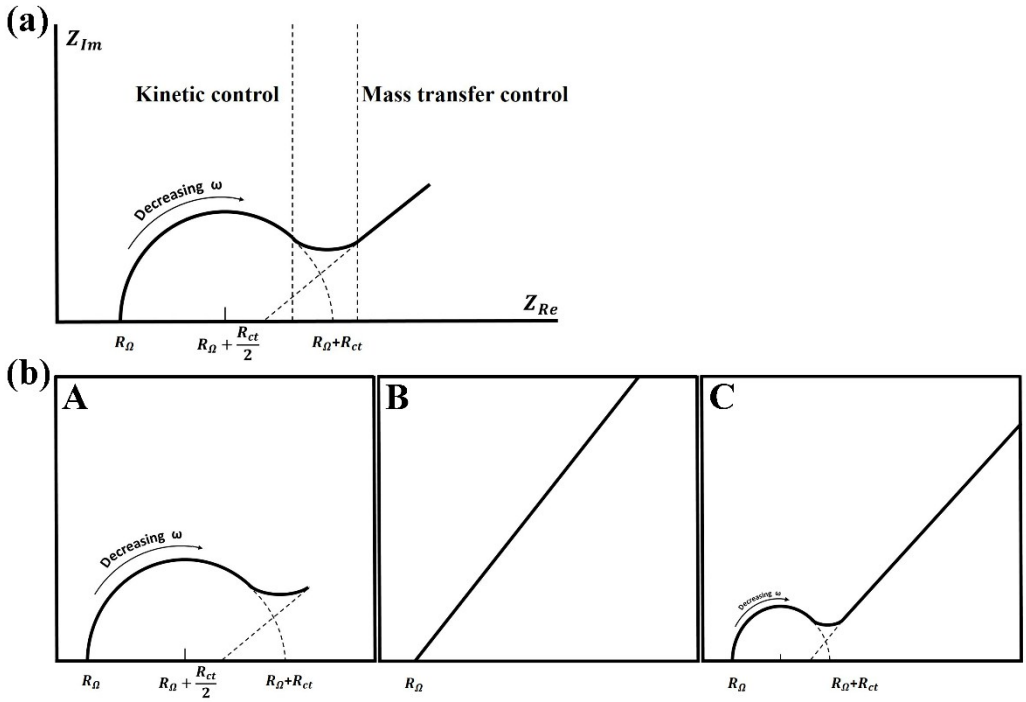

Figure S7. (a) Impedance plot for a common electrochemical system, regions of mass-transfer and kinetic control are found at low and high frequencies, respectively. (b) Three different situations for a specified electrochemical system.

The EIS analysis of 3DCS/P electrodes with different PANI thickness: The electrochemical system is described theoretically in terms of an equivalent circuit such as that in Figure S6, and an simulate impedance plot for a common electrochemical system shows as in Figure S7a.[30] For a specified system, the following three different situations may occur (Figure S7b): (A) If the chemical system is kinetically sluggish, it will allow a large charge-transfer resistance R_{ct}, and may display only limited-frequency region where mass transfer is a significant factor; (B) At the other extreme, R_{ct} might be inconsequentially small by comparison to the ohmic resistance R_Ω and Warburg impedance Z_W, so the semicircular region is not well defined and the system is so kinetically facile that mass transfer always plays a role; (C) An actual impedance plot combine the features of the two limiting cases A and B, the system controlled by the kinetic and mass transfer together.[30] In Figure 5b, it is apparent that the R_{ct} of 3DCS/P2 and 3DCS/P3 can be ignored and increase significantly to 21.28 Ω (3DCS/P4) and 38.24 Ω (3DCS/P5) with the increase of PANI thickness. Therefore, we can conclude that the 3DCS/P2 and 3DCS/P3 are in accordance with the state represented by the B situation, and 3DCS/P4 and 3DCS/P5 are in accordance with the state represented by the C situation.

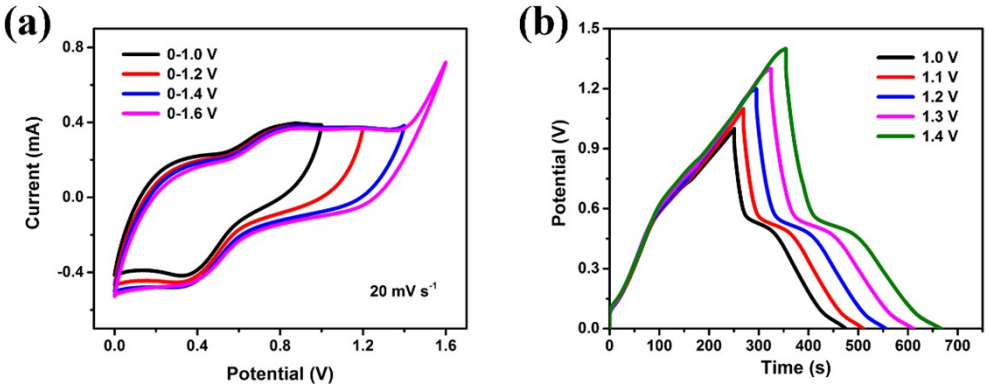

Figure S8. (a) The CV curves of 3DCS/P3//3DCS FASC device measured at different potential window at 20 mV s^{-1}. (b) Comparative GCD curves of FASC device at different potential window ranges.

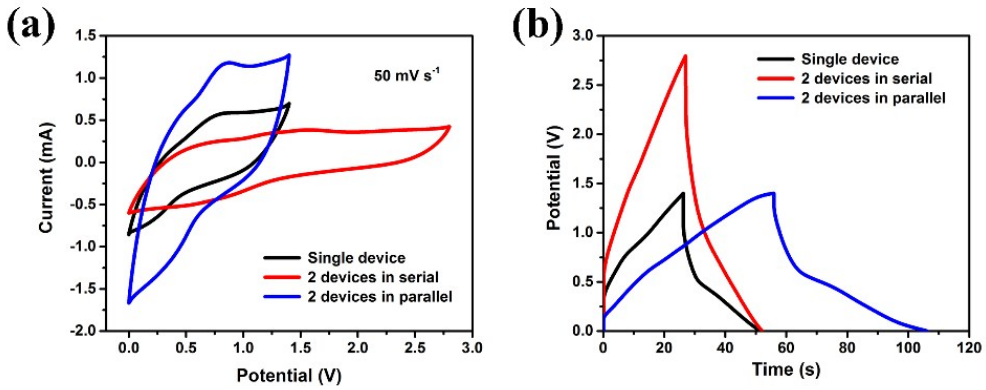

Figure S9. (a) CV and (b) GCD curves for two FASCs connected in series and parallel.

In fact, the working voltage and output capacity of a single SC may not be sufficient to power a practical electronic device. Two or more SCs could be connected in series or parallel to increase output voltage or power, respectively. Figure S9a shows the CV curves for two FASCs devices connected in series and parallel at a scan rate of 50 mV s^{-1}. By connecting two FASCs in series, the operating voltage is extended from 1.4 to 2.8 V, while retaining the original shape of CV curve. For the two FASCs in parallel, the CV curve gives an apparently larger area than that of the single device in the range of 0-1.4 V, suggesting that two FASCs in parallel can storage more charge compared to a single device at the same scan rate. Figure 9b shows the GCD curves performed on two devices connected in series and parallel at a current of 0.5 mA. The two serially connected FASCs were successfully charged to 2.8 V and the charge-discharge time is close to that of a single device. The charge-discharge time of two FASCs in parallel is more than two times that of the single device in the potential range of 0-1.4 V.

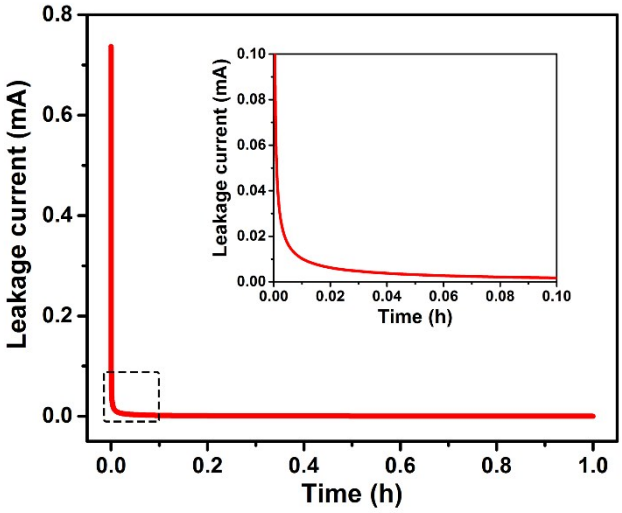

Figure S10. Specific capacitance based on the area and mass of the 3DCS/P3//3DCS FASC device versus current density.

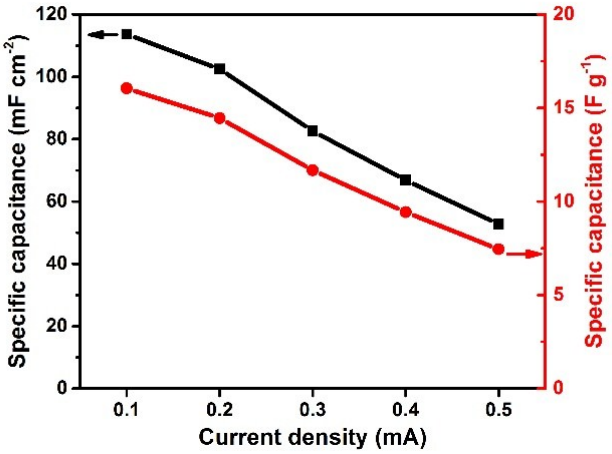

Figure S11. Specific capacitance based on the area and mass of the 3DCS/P3//3DCS FASC device versus current density.

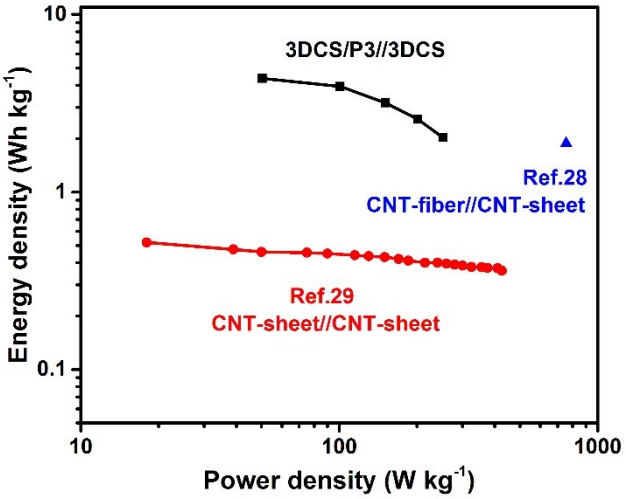

Figure S12. Ragone plot of 3DCS/P3//3DCS FASC device: E_i and P_i based on the total mass of the two electrodes and compares performance with those for the other fiber-shaped SCs.

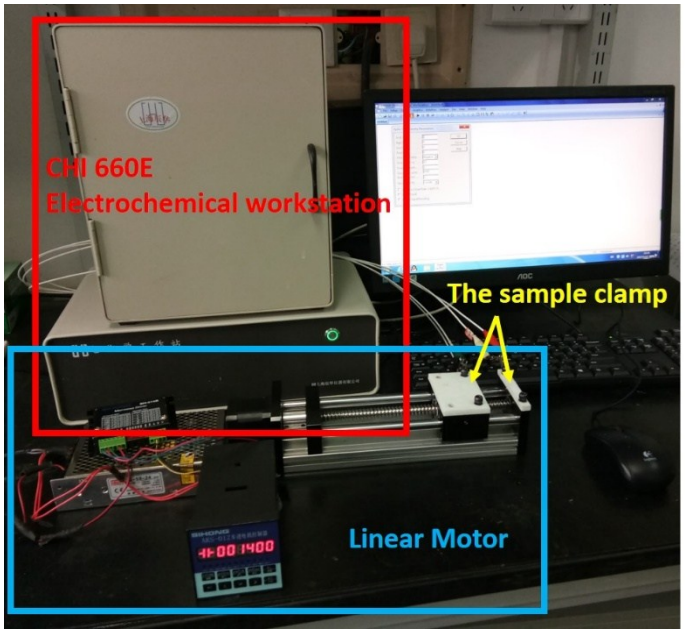

Figure S13. Photo of homemade integrated system for mechanical stability and electrochemical stability test.

3. Supplementary Tables

Table S1 Comparison of electrochemical performance for previous reported carbon/PANI composites.

Ref.	materials	C_m(F g^{-2})	C_l(F cm^{-1})	C_S(mF cm^{-2})	electrolyte	current density or scan rate
This	CNT/PANI	491.3	242.9	/	1 M H_2SO_4	~27 A g^{-1}

work						
47	CNT/PANI	/	/	680	1 M H_2SO_4	1 A g^{-1}
48	CNT/PANI	308.4	/	/	1 M H_2SO_4	1 A g^{-1}
49	CNT/PANI	501.8	/	/	0.5 M H_2SO_4	5 mV s^{-1}
50	Graphene/CNT/PANI	409	/	/	PVA/ H_2SO_4	10 A g^{-1}
51	3D-graphene/PANI	740	/	/	1 M H_2SO_4	0.5 A g^{-1}
52	Macroporous carbon/PANI	662	/	/	1 M H_2SO_4	1 A g^{-1}

Table S2 Comparison of the equivalent series resistance for previous reported fiber-shaped supercapacitors.

Device configuration	**Electrode material**	**Electrolyte**	**ESR**	**d**	**l**	**Ref.**
Twisted	3DCS/P//3DCS	PVA/H_2SO_4	287.4 Ω	/	/	This work
Twisted	CNT-fiber//CNT-fiber	PVA/H_2SO_4	7571.7 Ω	/	/	27
Twisted	CNT-fiber//CNT-fiber	PVA/H_3PO_4	~1100 Ω	/	/	28
Coaxial	CNT-fiber//CNT-sheet		~2000 Ω			
Twisted	RGO+CNT@CMC	PVA/H_3PO_4	550 Ω	/	/	33
	RGO@CMC		870 Ω			
	CNT@CMC		11220 Ω			
Twisted	CNT-fiber//CNT-fiber	PVA/H_2SO_4	~1000 Ω	/	/	34
	CNT@PANI//CNT@PANI		~1500 Ω			
Parallel	RGO-fiber//RGO-fiber	PVA/H_3PO_4	~2000 Ω	/	/	40
	RGO@MnO_2//RGO@MnO_2					
Parallel	PPy@MnO_2@CF	PVA/H_3PO_4	0.025 Ω cm^3	8 μm	3 cm	37
Twisted	CNT	PVA/H_2SO_4	~4 Ω cm^2	30 μm	1 cm	42
	CNT@NiO		~10 Ω cm^2			
	CNT@Co3O4		~14 Ω cm^2			

ESR is the equivalent series resistance of fiber-shaped supercapacitors; d and l is the diameter and length of the electrodes, and only marked when the symbol of ESR is Ω cm^3 or Ω cm^2.

Table S3 Electrochemical performances of recently reported fiber-shaped SCs.

Device configuration	Electrode material	Electrolyte	Structure	Voltage window	C_S/C_M	E_i	P_i	Ref.
Twisted	3DCS/PANI//3DCS	PVA/H_2SO_4	Asymmetric	0-1.4 V	113.64 mF cm^{-2} 16.05 F g^{-1}	30.92 μWh cm^{-2} 4.37 Wh Kg^{-1}	1.784 mW cm^{-2} 252 W Kg^{-1}	This work
Twisted	MnO2@ZnO@CNT//CNT	PVA/H_2SO_4	Asymmetric	0-1.6 V	46.08 mF cm^{-2}	20.7 μWh cm^{-2}	0.329 mW cm^{-2}	10
Parallel	N-doped RGO-SWCNT composite fiber	PVA/H_3PO_4	Symmetry	0.1 V	116.3 mF cm^{-2}	16.1 μWh cm^{-2}	2.84 mW cm^{-2}	14
Coaxial	MWCNT@CMF//CNT film	PVA/H_3PO_4	Symmetry	0-1 V	86.8mF cm^{-2}	9.8μW h cm^{-2}	189.4μW cm^{-2}	15
Twisted	PMMA@Au@ZnO@MnO_2	PVA/H_3PO_4	Symmetry	0-0.3 V	2.4 mF cm^{-2}	0.027 μWh cm^{-2}	0.014 mW cm^{-2}	17
Coaxial	Stainless steel wire@pen-ink//AC	PVA/H_3PO_4	Symmetry	0-0.8 V	3.18 mF cm^{-2}	/	/	18
Parallel	Au-wire@RGO	PVA/H_3PO_4	Symmetry	0-1.0 V	0.726 mF cm^{-2}	/	/	19
Parallel	Plastic wire/Au/pen ink	H_2SO_4	Symmetry	0-1.0 V	19.5 mF cm^{-2}	2.7 μWh cm^{-2}	9.07 mW cm^{-2}	20
Twisted	RGO-fiber//RGO-fiber	PVA/H_2SO_4	Symmetry	0-0.8 V	1.7 mF cm^{-2}	0.17 μWh cm^{-2}	0.1 mW cm^{-2}	25
Twisted	CNT-fiber//CNT-fiber	PVA/H_3PO_4	Symmetry	0-1 V	3.53 mF cm^{-2}	/	/	26
Twisted	CNT fiber/MnO_2	PVA/H_3PO_4	Symmetry	0-1 V	3.57 mF cm^{-2}	/	/	26
Twisted	CNT fiber	PVA/H_2SO_4	Symmetry	0-0.8 V	4.28 mF cm^{-2}	0.226 μWh cm^{-2}	0.493 mW cm^{-2}	27
Coaxial	CNT-fiber//CNT sheet	PVA/H_2SO_4	Symmetry	0-1 V	8.66 mF cm^{-2}	1.88 Wh Kg^{-1}	755.9 W Kg^{-1}	28
Coaxial	CNT sheet	PVA/H_3PO_4	Symmetry	0-0.8 V	20 F g^{-1}	0.515 Wh Kg^{-1}	421 W Kg^{-1}	29
Twisted	OMC-MWCNT composite fiber	PVA/H_3PO_4	Symmetry	0-1 V	39.7 mF cm^{-2}	1.77 μWh cm^{-2}	0.032 mW cm^{-2}	31
Parallel	SWCNT-AC composite fiber	PVA/H_2SO_4	Symmetry	0-0.8 V	37.1 mF cm^{-2}	3.29 μWh cm^{-2}	3.36 mW cm^{-2}	32
Twisted	RGO-CNT@CMC	PVA/H_3PO_4	Symmetry	0-0.8 V	/	3.84 μWh cm^{-2}	0.02 mW cm^{-2}	33
Twisted	PANI-NWs@CNT yarns	PVA/H_2SO_4	Symmetry	0-0.8 V	38 mF cm^{-2}	/	/	34
Twisted	MnO_2@rGO fiber	PVA/H_2SO_4	Asymmetric	0-0.8 V	9.6 mF cm^{-2}	/	/	38
Parallel	MnO_2@graphene	PVA/H_3PO_4	Symmetry	0-1 V	10.5 mF cm^{-2}	1.46 μWh cm^{-2}	0.69 mW cm^{-2}	40
Parallel double	MnO_2@Ti wire	PVA/LiCl	Symmetry	0-0.8 V	15.6 mF cm^{-2}	1.39 μWh cm^{-2}	579μW cm^{-2}	41

helix								